Heat treatment effects on the characteristics and sonocatalytic performance of TiO$_2$ in the degradation of organic dyes in aqueous solution

Ahmad Zuhairi Abdullah*, Pang Yean Ling

School of Chemical Engineering, Universiti Sains Malaysia, Nibong Tebal, 14300 Penang, Malaysia

ARTICLE INFO

ABSTRACT

The ambient sonocatalytic degradation of congo red, methyl orange, and methylene blue by titanium dioxide (TiO$_2$) catalyst at initial concentrations between 10 and 50 mg/L, catalyst loadings between 1.0 and 3.0 mg/L and hydrogen peroxide (H$_2$O$_2$) concentrations up to 600 mg/L is reported. A 20 kHz ultrasonic processor at 50 W was used to accelerate the reaction. The catalysts were exposed to heat treatments between 400 and 1000 °C for up to 4 h to induce phase change. Sonocatalysts with small amount of rutile phase showed better sonocatalytic activity but excessive rutile phase should be avoided. TiO$_2$ heated to 800 °C for 2 h showed the highest sonocatalytic activity and the degradation of dyes was influenced by their chemical structures, chemical phases and characteristics of the catalysts. Congo red exhibited the highest degradation rate, attributed to multiple labile azo bonds to cause highest reactivity with the free radicals generated. An initial concentration of 10 mg/L, 1.5 g/L of catalyst loading and 450 ppm of H$_2$O$_2$ gave the best congo red removal efficiency of above 80% in 180 min. Rate coefficients for the sonocatalytic process was successfully established and the reused catalyst showed an activity drop by merely 10%.

© 2009 Elsevier B.V. All rights reserved.

1. Introduction

Presently, it is estimated that about 10,000 different types of commercial dyes and pigments exist and over 700,000 tones are produced annually [1,2]. About 10–20% of the total world production of dyes is lost during the dyeing process and is released into the effluents [3]. Industrial dyestuffs constitute one of the largest groups of organic compounds that cause an increasing environmental concern [4]. Therefore, a lot of studies have been dedicated to treat this wastewater by using advanced oxidation process which involves hydroxyl (•OH) radicals to mineralize the organic compounds. Different degrees of success have been reported but the methods could subject to some common drawbacks like high capital and running costs, the needs for toxic chemicals and low removal efficiency, especially at low concentrations. Photocatalytic degradation is another plausible method but its practicality is generally limited with heavily colored effluent, high photocatalyst loading and high volume operation due to low penetration of the UV light [3,4].

The application of ultrasounds in water with a frequency range of between 18 and 100 MHz can result the phenomenon of acoustic cavitation. It involves the formation, growth and collapse of cavity bubbles that entrapped dissolved gases or vapors surrounding

water [5,6,7]. Subsequently, many local hot spots with extremely high temperature (up to 5000 K) and high pressure (up to 1000 atm) are generated to consequently induce the dissociation of water (Eqs. (1)–(4)), oxygen molecules (Eqs. (5)–(8)) and hydrogen peroxide (H$_2$O$_2$) (Eq. (9)) in the case of its addition into the effluent [5,7,8].

$$H_2O \xrightarrow[\text{TiO}_2]{))))} \cdot OH + H\cdot \tag{1}$$

$$\bullet OH + H\bullet \rightarrow H_2O \tag{2}$$

$$2\bullet OH \rightarrow H_2O_2 \tag{3}$$

$$2\bullet OH \rightarrow H_2O\bullet + O\bullet \tag{4}$$

$$O_2 \xrightarrow[\text{TiO}_2]{))))} 2O\cdot \tag{5}$$

$$\bullet O + H_2O \rightarrow 2\bullet OH \tag{6}$$

$$O_2 + H\bullet \rightarrow \bullet O_2H \tag{7}$$

$$\bullet O_2H + \bullet O_2H \rightarrow H_2O_2 + O_2 \tag{8}$$

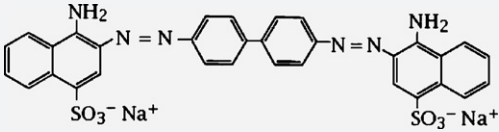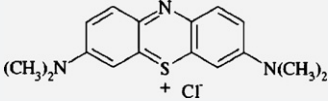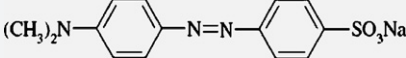$$H_2O_2 \xrightarrow[\text{TiO}_2]{))))} 2 \cdot OH \tag{9}$$

As a semiconductor material, TiO$_2$ is characterized by a filled valence band and an empty conduction band [3,4]. In the presence of suitable energy source, the excitation of electron from the valence band to the conduction band could occur. With the presence of UV light or ultrasonic irradiation as the energy source,

* Corresponding author. Tel.: +60 4 599 6411; fax: +60 4 594 1013.
E-mail address: chzuhairi@eng.usm.my (A.Z. Abdullah).

Table 1
Structures and molecular weights of congo red, methylene blue and methyl orange dyes.

Dyes	Chemical structure	Molecular weight (g/mol)
Congo red		696.67
Methylene blue		373.88
Methyl orange		327.34

electron (e^-) can be promoted from the valence band into the conduction band, leaving a hole (h^+) behind by furnishing energy matching or exceeding the band gap energy of the catalyst. The holes are responsible for the accelerated dissociation of water molecules to form hydroxyl free radicals that in turn, involved in the degradation of organic pollutants in the water [6,7]. Thus, the presence of TiO_2 can significantly accelerate the generation of hydroxyl free radicals as compared to that caused by the sonolysis of water molecule alone. The ultrasonic irradiation could overcome the main drawback of UV light i.e. low penetration rate in heavily colored solutions and shielding effects by the particles in the water. The presence of TiO_2 particles in the liquid also increases the nucleation sites for cavity formation, resulting in the generation of more free radicals. The accelerated generation of hydroxyl free radical in the TiO_2 sonocatalytic reaction has been studied and proven by Shimizu et al. [9] by examining the oxidation of salicylic acid.

Different phases of TiO_2 behave differently in the case of photocatalysis and generally anatase phase is desirable [3]. In the case of sonocatalytic process, rutile is reported to be more active for the degradation of basic blue 41 dye [4] and methyl parathion [6]. Therefore, it is of great interest to know whether the same conclusion can be extended to other organics as well. The transformation of anatase to rutile and possibly brookite usually takes place at high temperature (>700 °C) and corresponding changes in the physical properties apart from the phase change could also result. The combined changes will certainly affect the sonocatalytic activity and the other process behaviors and the optimum conditions for the treatment should be clearly identified. This aspect of the sonocatalytic process receives little attention until very recently and usually researchers use a pure form of specific TiO_2 phases as the sonocatalyst as reported by Wang et al. [3].

In this study, titanium dioxide (TiO_2) catalyst has been used as the sonocatalyst for many advantages such as inexpensive, nontoxic, stability and reusability [4,10]. In its presence, the increase the rate of formation •OH radicals will result to consequently accelerate the degradation of organic pollutants in the water [11]. Congo red, methyl orange and methylene blue have been used as the model organic dyes to be degraded and further information on the dyes are given in Table 1. The study is mainly dedicated to the effects of various heat treatments on the characteristics of the TiO_2 sonocatalysts and their consequent effects on the catalytic activity. The behaviors observed have been related with the molecular weight, type of chemical bond and structure of the dye molecules as well as the characteristics of the TiO_2 catalyst itself. The process behaviors under various operating conditions have been elucidated while further process acceleration with the addition of H_2O_2 and its potential to be reused has also been demonstrated. In addition, a simple yet reliable kinetic model has been introduced to represent the sonocatalytic reaction. Its applicability to sonolytic, sonocatalytic and hydrogen peroxide-assisted sonocatalytic systems has also been

explored. An attempt has also been made to study the changes in the particle size distribution of the TiO_2 after the sonocatalytic reaction.

2. Experimental

2.1. Materials

Anatase TiO_2 powder (R & M, U.K.) was used as the sonocatalyst with and without heat treatment. H_2O_2 at a concentration of 30% (Merck Bchuchardt OHG) was used as a promoter for the sonocatalytic degradation process. Congo red, methyl orange and methylene blue powders (R & M Marketing, Essex, U.K.) were used as model organic compounds for the demonstration of the sonocatalytic activity of heat-treated TiO_2 sonocatalysts.

2.2. Preparation and characterization of the heat-treated TiO_2 sonocatalysts

Six sets of 15 g TiO_2 powders were weighted and heat-treated at various temperatures (400–1000 °C) and durations (2 and 4 h) in a muffle furnace to induce phase transformation. X-ray diffraction (XRD) pattern of the original and heat-treated TiO_2 powders was determined using a Bruker D8 diffractometer in order to study the effect of temperature on the extent of phase transformation. The crystallite size (D) of anatase and rutile phases for the broadening of the diffraction peaks were calculated using the Scherrer relationship [12] i.e. $D = K\lambda/\beta\cos\theta$ where β is the full width at half maximum of the selected peak, θ is the Bragg's angle of diffraction for the peak and λ is the wavelength of the Cu-K$_\alpha$ radiation used i.e. 1.5405 Å. The weight fraction of anatase (W_A) and rutile (W_B) phases present in the TiO_2 sonocatalysts after various heat treatments was calculated using the equation generally reported [13–15] i.e. $W_A = [1 + 1.26(I_R/I_A)]^{-1}$ and $W_B = [1 + 0.8(I_A/I_R)]^{-1}$ where, I_A and I_R are the X-ray integrated intensities of reflection of anatase and rutile, respectively. The SEM pictures of the original and heat-treated TiO_2 powders were conducted for comparing the differences and changes between each of them. A Leica Cambridge S-360 scanning electron microscope (SEM) was used for this purpose. In addition, a CILAS 1180 series particle size analyzer was also used to further characterize the size distribution of the sonocatalysts.

2.3. Sonocatalytic reaction

A probe type ultrasonic processor (Branson, model 250) operated at a fixed frequency of 20 kHz and a full output power of 200 W was adopted to irradiate organic dye solutions. The desired output power was reduced to the desired value i.e. 50 W by adjusting the power level knob of the equipment until the right power output
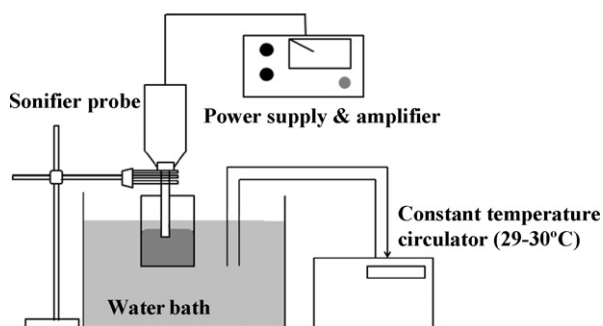
Fig. 1. Schematic diagram of the sonocatalytic experimental set up.

was displayed. An ultrasonic processor at this frequency has been reported to be successful in achieving significant degradation of surfactant and phenolic compounds in water within 2 h [16]. The general schematic diagram of experimental set up is illustrated in Fig. 1. In a typical experimental run, 100 mL of dyes solution was prepared in a 500 mL glass reaction vessel and TiO$_2$ sonocatalysts were then added. Then, the suspension was stirred for a while to ensure a good dispersion of the TiO$_2$ particles. The reaction vessel was then placed inside a water bath to maintain the temperature at around 30 °C. Next, the sonifier probe was inserted into the center of the vessel to provide ultrasonic irradiation. The main process variables adopted throughout the whole experiments were initial dyes concentration (10–50 mg/L), catalyst loading (1–3 g/L) and H$_2$O$_2$ concentration (0–600 mg/L) and the reaction was performed in neutral pH.

2.4. Reusability study of the TiO$_2$ sonocatalyst

After the reaction, the TiO$_2$ sonocatalyst was collected and washed at least three times with distilled deionized water and subsequently dried in an oven at 105 °C for 2 h. After that, the TiO$_2$ sonocatalyst catalyst was reused for the degradation of congo red at a concentration of 10 mg/L and a catalyst loading of 1.5 mg/L.

2.5. Analysis of liquid samples

After the desired reaction times, 10 ml of liquid samples were taken out from the reaction vessel and a centrifuge (Kubota 2100) operated at 3500 rpm for 10 min was used to remove any suspended TiO$_2$ powders. Insignificant amount of dyes in the solution was expected to be removed during this centrifugation process as all the dyes were completely soluble in the water. After that, the samples' dye concentration was measured using a PerkinElmer 950 UV–vis spectrophotometer. Measurement wavelengths of 666, 498 and 465 nm, respectively, were used for the determination of methylene blue, congo red and methyl orange concentrations, respectively. Below a dye concentration of 20 mg/L, the Beer–Lambert Law was found to be fully obeyed by all the dyes. The degradation efficiency is defined as;

$$\text{Degradation efficiency}(\%) = \frac{C_o - C_t}{C_o} \times 100\% \qquad (10)$$

where, C_o = initial dye concentration (mg/L) C_t = dye concentration at time t (min) (mg/L)

The method used in this study for the measurement of the dye concentration was deemed suitable and consistent with that reported literatures [3,4,6]. Abbasi and Asl [7] made an attempt to follow the changes in light absorbance from about 200 nm (UV region) 770 nm (visible region) during the sonocatalytic degradation of basic blue 41 dye. They came to the conclusion that the peak absorbance occurred at exactly the same wavelength and did not

change during the course of the reaction. Changes in the absorbance within the UV region were not expected to affect the accuracy of the measurement performed within visible range. In other words, degradation of the dye molecules led to its decolorization and no significant amount of visible light absorbing species were created during the reaction. No COD, TOC, HPLC or ion chromatograph tests were conducted in this study as the scope was only to study the degradation efficiency rather than the mineralization of the dyes.

3. Results and discussions

3.1. XRD and SEM of TiO$_2$ powders

Fig. 2 shows the XRD patterns of the original and various heat-treated TiO$_2$ powders. As expected, the original TiO$_2$ sample was in anatase form. Anatase phase of TiO$_2$ has been reported to be sufficiently active for the sonocatalytic degradation of rhodamine B and rhodamine blue dyes [17]. At a calcination temperature of 400 °C, a tiny peak associated with the orthorhombic brookite phase appeared and it quickly disappeared at higher temperatures. A new peak ascribed to the tetragonal rutile phase was observed after a heat treatment above 800 °C. This result was in agreement with reported results saying the transformation of anatase to rutile is only possible at above 700 °C [3,15]. Below the critical temperature for the transformation, increasing the duration of the treatment did not bring any effect on the phase transformation to metastable rutile phase [12,15]. However, the critical temperature for the transformation was not able to be accurately determined in this study due to the wide temperature interval used (200 °C). The peak intensity showed a slight increase with the doubling of treatment time at 800 °C but doing the same at 1000 °C resulted in the significant appearance of rutile phase. For the TiO$_2$ sample treated at 1000 °C for 4 h, significant transformation to rutile was detected based on the intensity and appearance of multiple diffraction peaks associated with the TiO$_2$ phase.

The calculated values of phase composition for anatase, brookite and rutile phases are presented in Table 2 based on the intensities observed from Fig. 2. As the calcinated temperature was increased from 800 °C (2 h) to 1000 °C (4 h), the composition of rutile phase was detected to increase from 5.7% to 27.7% with a corresponding increase in the average crystal size. It was therefore concluded that the high temperature calcination would greatly affect the phases and the size of the TiO$_2$ crystal. The crystal sizes for both anatase and rutile increased with increasing of calcination temperature, indicat-
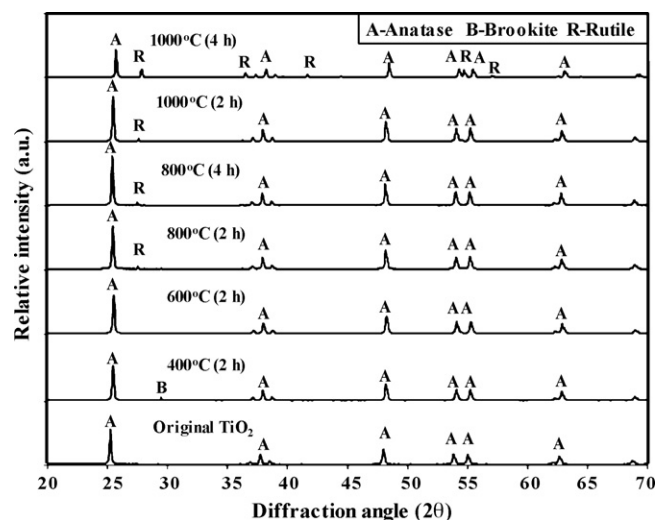

Fig. 2. XRD patterns of the original and various heat-treated TiO$_2$ powders.

Table 2
XRD results of the original and heat-treated TiO_2 powders.

Calcination temperature (°C) and duration	Average crystal size (nm)			Phase composition (%)		
	Anatase	Brookite	Rutile	Anatase	Brookite	Rutile
Original	56.0	–	–	100.0	–	–
400, 2 h	55.5	65.8	–	98.2	1.8	–
600, 2 h	53.6	–	–	100.0	–	–
800, 2 h	63.0	–	18.1	94.3	–	5.7
800, 4 h	66.2	–	33.3	95. 3	–	4.7
1,000, 2 h	61.6	–	27.4	93.8	–	6.2
1,000, 4 h	62.2	–	52.8	73.3	–	27.7

ing that the high temperature would promote crystallite growth or aggregation of TiO_2 particles. Similar observation has been reported by Kumar [12] for titania–alumina composite material. As the calcination temperature was increased from 800 to 1000 °C, the average crystal size of the rutile phase almost doubled from 33.3 to 52.8 nm. The crystallite size of the anatase phase increased from 56.0 to 62.2 nm when calcined at 1000 °C for 4 h.

Thus, the increasing temperature and the duration of heat treatment would accelerate phase transformation from thermodynamically metastable (anatase) to most stable and more condense rutile phase. The rutile started to appear when high temperature was used to give TiO_2 sonocatalysts with mixed phases to be subsequently used in the sonocatalytic degradation process. However, other physical changes must have occurred beside the phase transformation to affect the sonocatalytic behavior [15]. Therefore, it was of great interest to further characterize the sonocatalysts for the surface and grain characteristics.

Fig. 3 shows the SEM images the original and various treated TiO_2 particles. The TiO_2 powders that were calcined in a range

of 400 °C to 800 °C (Fig. 3b–d) show no obvious difference on the size of the agglomerates as compared to those of untreated TiO_2 (Fig. 3a). They generally consisted of spherical particles and many micro and mesopores were expected at the interstices of the particles. It can be seen that as the annealing temperature was increased, the size and shape of these spherical particles remained unchanged for almost up to 800 °C. With a further increase of calcination temperature, the particles aggregated to form larger particles with relatively smoother surfaces. Significant agglomeration between these spherical particles was observed only for the case of TiO_2 powders that was heat-treated at a temperature of 1000 °C for 2 h (Fig. 3e) and more distinctly in the sample that was heated at 1000 °C for 4 h (Fig. 3g). It is noted that the micro and mesopores at the interstices of the particles were significantly reduced, especially after the extreme heat treatments at 1000 °C.

Porter et al. [18] observed that the grain size of Degussa P-25 TiO_2 powders increased by a factor of nearly 10 when the calcination temperature was increased from 600 to 900 °C for 3 h. However, in the present work, such a rapid grain growth was
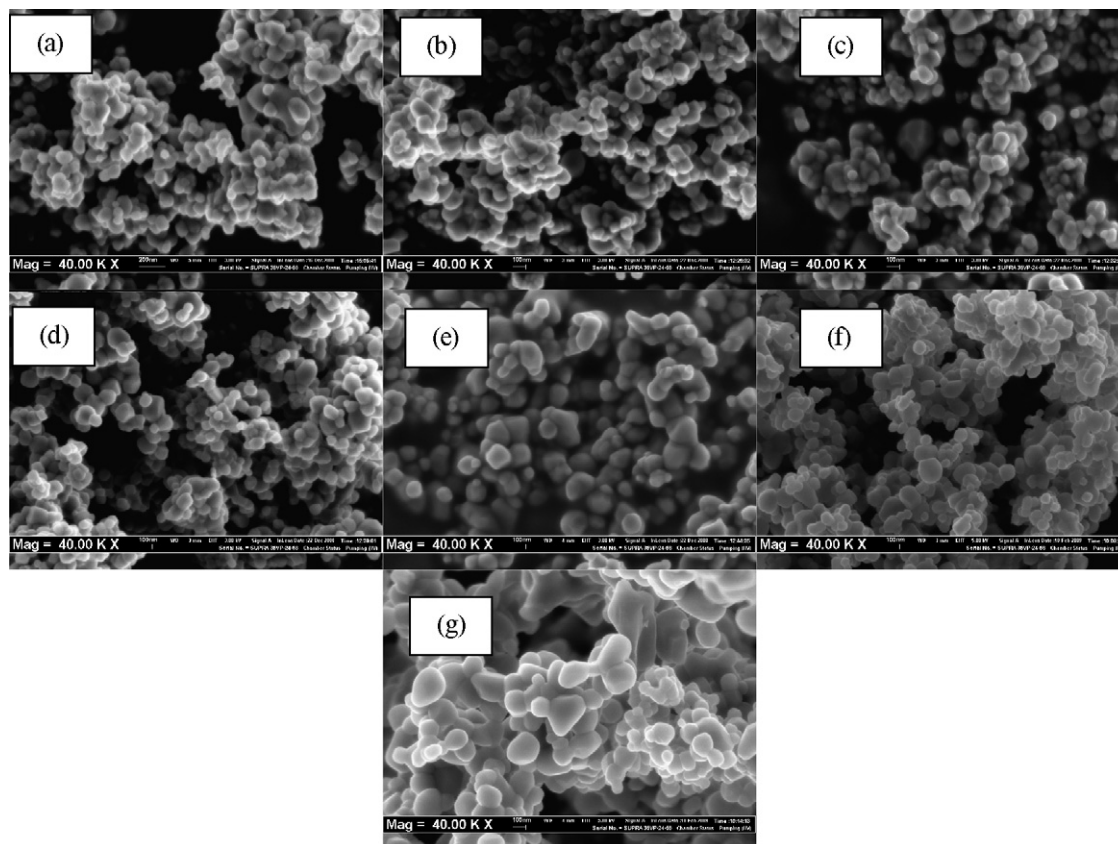

Fig. 3. SEM images of the particles of (a) original TiO_2, (b) heat-treated TiO_2 at 400 °C for 2 h, (c) heat-treated TiO_2 at 600 °C for 2 h, (d) heat-treated TiO_2 at 800 °C for 2 h, (e) heat-treated TiO_2 at 1000 °C for 2 h, (f) heat-treated TiO_2 at 800 °C for 4 h and (g) heat-treated TiO_2 at 1000 °C for 4 h.

not observed when calcinations of up to 1000 °C for 4 h were performed. Besides, Kim and Hahn [19] observed that as the nanocrystalline TiO$_2$ particles were calcinated at about 600 °C, anatase crystals within agglomerates became sintered, thus the crystals size grew through the coalescence. Thereby, it transformed the original agglomerates into single anatase grains. Thus, the results in the present study were consistent with the reported results.

3.2. Effect of different chemical structures of dye and heat-treated catalysts

In this study, the removal of dyes was confirmed by the significant drop in the absorbance in visible wavelength with time as shown in Fig. 4. Besides, changes in the UV region were also noticeable for all dyes to give the indication that new products
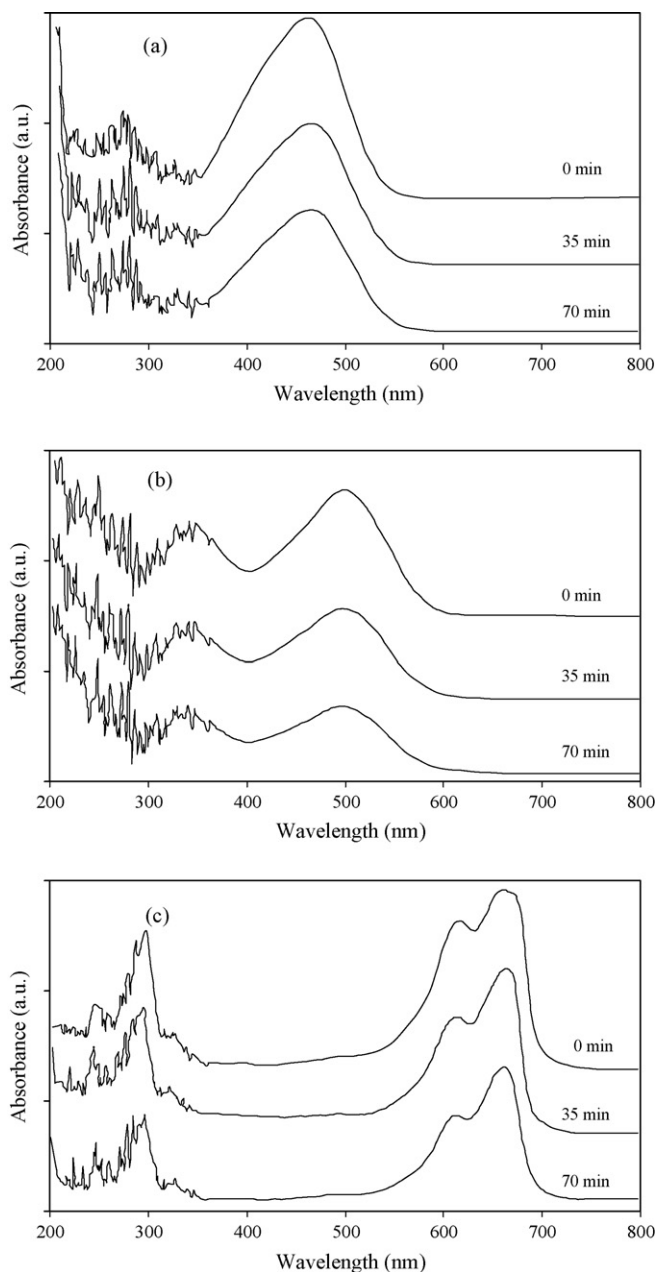

Fig. 4. Changes in the absorbance during the degradation of (a) methyl orange, (b) congo red and (c) methylene blue dyes. (Initial dye concentration = 20 mg/L, catalyst loading 2.0 g/L).
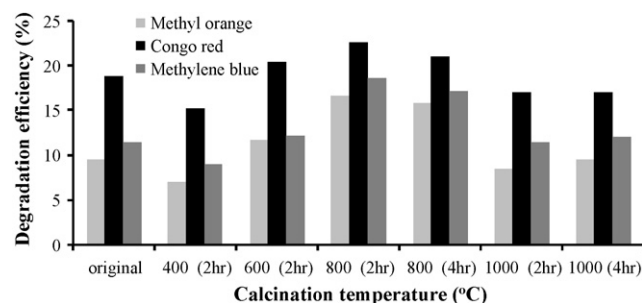

Fig. 5. Degradation efficiency of various dyes during the sonocatalytic process by different catalysts. (Initial dye concentration = 20 mg/L, catalyst loading 2.0 g/L, reaction time = 75 min).

were formed during the reaction. This observation was attributed to the degradation of the dye molecules to form small (colorless) degradation products such as aldehydes and organic acids that are usually absorbing in UV wavelengths (200–400 nm). This observation confirmed that the removal of the dyes was indeed caused by the degradation of the organic substances. However, specific trend was not observed as the ultimate gaseous and volatile products would simply escape from the reaction mixture. In the degradation of large molecules such as the three dyes, numerous degradation products will be produced so that the identification of specific products is deemed unnecessary. The degradation efficiencies for three types of dyes after 75 min of ultrasonic irradiation using 2.0 g/L of catalyst are shown in Fig. 5. The dyes degradation efficiency with all the sonocatalysts generally followed the order as below:

Congored > methyleneblue > methyl orange

Consistent behavior of the sonocatalytic degradation process with all the sonocatalysts suggested that the behavior was mainly influenced by the molecular structures of the organic rather than the characteristics of the sonocatalysts. This sonocatalytic behavior is also shared by phenolic compounds [17]. The low stability of the congo red was attributed to the presence of 2 azo (–N=N–) labile bonds its large molecule that were generally more susceptible to attack by free radicals during the reaction. Meanwhile, methylene blue and methyl orange are of almost similar molecular size. However, the former dye showed lower stability due to the presence of one charged sites in the ring while that of methyl orange located at the external of the ring. In this respect, similar result was reported by Lachheb et al. [20] for the case of photocatalytic degradation by using anatase of TiO$_2$. They found that the degradation efficiency decreased from congo red to methylene blue, then crocein orange G. Thus, some similarities between the sonocatalytic and photocatalytic degradation processes were demonstrated in this study. Hachem et al. [21] reported that the photocatalytic degradation efficiency of congo red was higher than that of remazol blue, orange II or orange G. The stability of the dyes was greatly associated with molecular weight and types of bond present in the dyes.

The rate of reactivity of •OH radicals with the dye molecules needs to be determined to compare the degradation rate among different structures of dye. Azo bonds or azobenzene (chromophore for congo red and methyl orange) generally have the higher reactivity coefficient with •OH radical than dimethylamine group (auxochromes for methyl blue and methyl orange) which was reported to accelerate the rate of degradation. The reactivity coefficient of azobenzene, dimethylamine, benzenesulfunic acid and benzene ring are given as below [22].

$$k_{azobenzene}^{\cdot OH} = 2.0 \times 10^{10} \text{ L/mol/s} \tag{11}$$

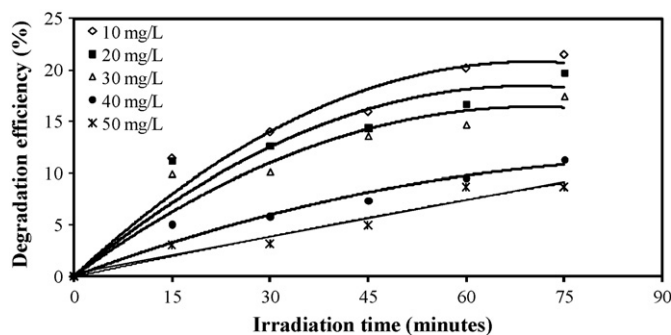$$k_{dimethylamine}^{\cdot OH} = 1.4 \times 10^{10} \text{ L/mol/s} \tag{12}$$

Fig. 6. Effect of initial dye concentration on the sonocatalytic degradation of congo red dye. (Catalyst loading = 2.0 g/L).

$$k_{benzenesulfunic\ acid}^{\bullet OH} = 2.1 \times 10^9 \text{ L/mol/s} \tag{13}$$

$$k_{benzene}^{\cdot OH} = 1.7 \times 10^9 \text{ L/mol/s} \tag{14}$$

Thus, congo red dye which contains two azo groups would possess higher reactivity with •OH radicals, followed by methylene blue and methyl orange. By considering all the rates of reactivity to •OH, peroxyl (HO$_2$•) and super peroxide radicals (O$_2^{-}$•) with respect to the compound in the dye structure, it could be concluded that the rate of degradation in congo red was relatively more rapid, followed by that of methylene blue and methyl orange.

Also noted in Fig. 5, the highest degradation efficiency was obtained when the TiO$_2$ was heat-treated at a temperature of 800 °C for 2 h. This observation indicated that such heat-treated TiO$_2$ powder possessed the highest sonocatalytic activity. Recalling that the rutile phase was significantly present in this TiO$_2$ sonocatalyst while the micro and mesoporousity were maintained in the particles, the highest degradation efficiency was associated with the combined effect of these factors. Rutile phase with appropriate area and thickness on the surface of anatase phase is reported to have the ability to inhibit the recombination of e^{-}–h^{+} pairs [12]. However, excessive heat treatment would also result in the agglomeration of the particles causing the loss of porosity to consequently limit the capability of the TiO$_2$ sonocatalyst to generate free radicals. In this case, rutile phase embedded within the catalyst particles were unavailable for contact with the solution to catalyze the degradation reaction.

3.3. Effect of initial dye concentration

As congo red showed the highest removal efficiency in the sonocatalytic process, it was used for the further demonstration of the effect of various process variables. TiO$_2$ that was treated at 800 °C for 2 h was used as the sonocatalyst due to the highest activity as shown in Fig. 5. Fig. 6 shows that the degradation efficiency of the sonocatalytic system with a catalyst loading of 2.0 g/L decreased with the increasing initial congo red concentration from 10 to 50 mg/L. In this respect, the sonocatalytic degradation process showed some similarities with those of a photocatalytic process [21]. Therefore, it could be concluded that the course of reaction in the two processes was almost similar. The major difference was the mechanism to the initiation of the reaction through the formation of free radicals.

There are two possible reasons for the experimental observation. Firstly, high initial concentration of dye solution caused more degradation to take place to achieve the same level of degradation (expressed as percent reduction). However, higher concentration might also cause excessive adsorption of the congo red molecules on the surface of TiO$_2$ powder on the TiO$_2$ sonocatalyst to limit its efficiency [18]. Also, mutual screens between congo red molecules and TiO$_2$ particles increased with increasing the initial dye concen-
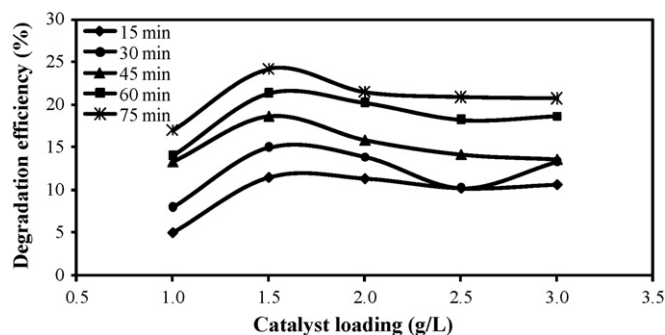

Fig. 7. Effect of TiO$_2$ catalytic loading on the sonocatalytic degradation of congo red dye at a concentration of 10 mg/L.

tration to result in the same effect. These two phenomena would prohibit TiO$_2$ particles from absorbing heat and energy released from the acoustic cavitation and also disturbed the transmission of ultrasound. This would consequently limit the generation of •OH radicals leading to a decrease in the degradation efficiency.

3.4. Effect of TiO$_2$ loading

Fig. 7 shows a series of experiments done by varying the loading of TiO$_2$ from 1.0 to 3.0 g/L in order to obtain the optimum loading. The degradation efficiencies were determined at various reaction times of between 15 and 75 min. Results show that the degradation efficiency of congo red rose significantly when the TiO$_2$ loading was increased from 1.0 to 1.5 g/L. The effect was attributed to the increasing sites to generate free radicals with the increasing sonocatalyst loading [11]. The removal efficiency began to decline at higher loadings and the same trend was shared by all the reaction times tested. Also, longer reaction times resulted in higher efficiency for all the loadings to correctly show the behavior of a non-reversible reaction.

The lower removal at high loadings could be explained by the fact that the excessive TiO$_2$ particles could cause mutual screening effects between the particles that that would shield congo red molecules from receiving sonic waves. Below a catalyst loading of 1.5 g/L, the shielding effect was not detected at the degradation efficiency increased with loading. The effect was only found to significantly occur at higher loadings (2.0–3.0 g/L) as the degradation efficiency was observed to level off or decrease with increasing catalyst loading. The same behavior was observed at different reaction times to the agreement with this argument. The shielding effect would eventually prohibit TiO$_2$ particles from absorbing heat and energy resulting from the acoustic cavitation [23]. Consequently, it might result in a reduction in the rate of •OH generation. The same phenomenon was reported in photocatalytic reaction but the optimum catalyst loading occurred at lower values [10]. Thus, sonocatalytic allows higher loading of TiO$_2$ to be used to achieve higher degradation efficiency of the target organic pollutants.

3.5. Effect of the addition of H$_2$O$_2$

H$_2$O$_2$ has been reported to promote the photocatalytic degradation of monochlorobenzene [10], crocein orange G and alizarin S [20], and several other dyes [21]. Therefore, it is of great interest to learn whether the same behavior could be shared in the case of sonocatalytic process. The addition of H$_2$O$_2$ at various concentrations (up to 600 mg/L) was carried out in this study for the purpose of initiating and promoting the free radical generations. Below equations show that the H$_2$O$_2$ molecule acting as a hydroxyl scavenger (reaction 15) and as hydroxyl source (reaction 16) under
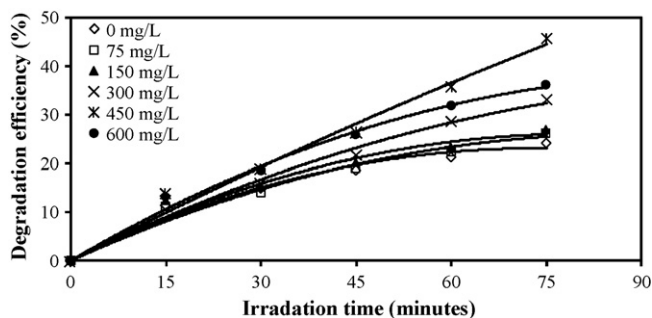
Fig. 8. Effect of the addition amount H_2O_2 on the sonocatalytic degradation of congo red (initial dye concentration = 10 mg/L, TiO_2 amount = 1.5 g/L).

sonocatalytic condition [24].

$$H_2O_2 + {}^\bullet OH \rightarrow H_2O + HO_2{}^\bullet \qquad (15)$$

$$H_2O_2 + {}^\bullet H \rightarrow {}^\bullet OH + H_2O \qquad (16)$$

As noted in Fig. 8, the amount of H_2O_2 added had a positive contribution on the degradation of congo red up to a concentration of 450 mg/L. Further increase in the concentration of H_2O_2 to 600 mg/L caused a detrimental effect to the reaction. Thus, the promotion of the free radical formation as given in Eqs. (15) and (16) was just limited to below 450 mg/L for this concentration of dye. Reduced removal efficiency at a H_2O_2 concentration of 600 mg/L was attributed to the fact that at high concentration, H_2O_2 would become a scavenger to $^\bullet OH$ radicals [7,14]. $^\bullet OH$ and $H^\bullet$ radicals were generated by the dissociation of water (as given by Eq. (1)) and excess H_2O_2 could scavenge the $^\bullet OH$ radicals produced to handicap the subsequent degradation reactions. Almost similar behavior was reported for the photocatalytic degradation of various dyes [20] and sonocatalytic degradation of parathion [23]. That would result in a lower degradation of the dye in the solution. However, the optimum concentration of H_2O_2 found in this study was significantly lower (1700 versus 450 mg/L as used in this study) than that used in the sonocatalytic degradation of methylene blue as reported by Shimizu et al. [11]. Perhaps, the result reported by them was not obtained under optimum condition with respect to the H_2O_2 concentration.

3.6. Effect of various conditions on degradation congo red by stirring or ultrasonic irradiation

The experimental results for relationships between degradation efficiency of congo red with time under ultrasonic irradiation or mechanical stirring for 180 min are shown in Fig. 9. As a background study, mechanical stirring (denoted 'stir' in the figure) and the subsequent centrifugation step did not result in any decrease
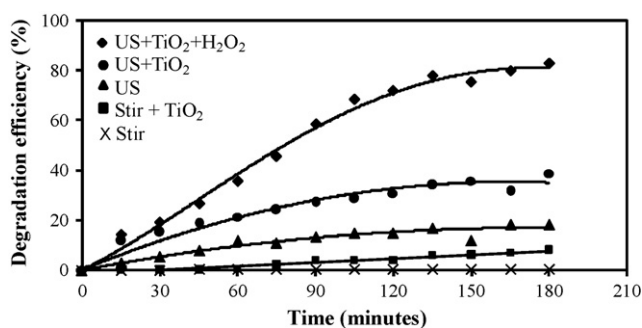

Fig. 9. Profiles of congo red degradation efficiency versus reaction time under various conditions (initial dye concentration = 10 mg/L, TiO_2 loading = 1.5 g/L, 450 mg/L of H_2O_2).

in the dye concentration. Small reduction with presence of TiO_2 was attributed to some dye adsorption on the material. The occurrence of dye adsorption was also reported in the photocatalytic degradation process [20]. Ultrasonic treatment alone resulted in a reduction of up to 10% due to the sonolysis of the dye molecules. Thus, it could be concluded that the dissociation of water molecules could also occur without the presence of TiO_2, to the agreement with a reported result using an ultrasonic irradiation at 35 kHz for the degradation of basic blue 41 dye [7]. However, it would be significantly accelerated when the catalyst was present as suggested by the sonocatalytic result (US + TiO_2). Drastic increase in the efficiency resulted when 450 mg/L of H_2O_2 was used.

Results in Fig. 9 prove the suitability of the experimental procedure used to study the degradation of dye. The blank experiments didn't result in any removal while the contribution of adsorption on the TiO_2 particles was just limited to about 4%. This slightly lower than that reported in the case of photocatalytic [21] and the result could be associated with the mechanical effects caused by the ultrasonic irradiation. The contribution of sonolysis was limited to about 15% and further degradation was contributed to catalytic activity. Wang et al. [23] reported higher contribution of sonolysis in the case of methyl parathion degradation at 80 kHz. Therefore, the extent of sonolysis could be influenced by the ultrasonic frequency used and the molecular structure of the organic itself.

In the case of H_2O_2 assisted sonocatalytic degradation of congo red, it could be concluded that the supplementary of free radicals on top of those generated by the dissociation of water was beneficial to the process. In this case, almost 80% of congo red degradation efficiency was achieved in 180 min under the optimum conditions (10 mg/L of dye solution, 1.5 g/L of TiO_2 loading and 450 mg/L of H_2O_2). This result indicates the enhancement in degradation efficiency of congo red was about twice higher than that of sonocatalytic alone. In this case, the higher concentration of radicals resulted in their more efficient reaction with the organics in the water. Usually, the radicals react with dissolved organic compounds by hydroxylation and will undergo further oxidation in presence of oxygen in the dissolved [25]. In the case of very fast reaction, oxygen supplement could be necessary to allow complete mineralization of the organic [21].

3.7. Study on degradation reaction kinetics

In order to determine the order of the reaction for the sonocatalytic degradation of congo red, kinetic studies were performed on the basis of the rate of disappearance of the dye. Several orders such as zero, first, second orders graph were considered for the experimental data obtained using congo red dye at an initial concentration of 10 mg/L. Three cases considered were the sonolysis (without TiO_2), sonocatalytic (with TiO_2) and H_2O_2 accelerated sonocatalytic (with TiO_2 and H_2O_2). Based on the evaluation done, only a simplified pseudo first-order kinetics satisfactorily fitted all the data while the other kinetics resulted in regression coefficients of lower than 0.6. The simplified rate expression for the reaction rate $(-r)$ sonocatalytic degradation of congo red dye by $^\bullet OH$ radical is given as below:

$$\text{Congo red}_{(aq.)} + {}^\bullet OH_{(aq.)} \rightarrow \text{ products} \qquad (17)$$
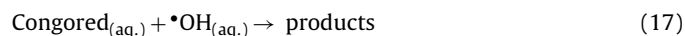
where the rate constants k' can be determined by;

$$-r = \frac{d}{dt}[\text{congo red}] = k'[\text{congo red}][{}^\bullet OH] \qquad (18)$$

As $^\bullet OH$ is a very reactive species, its concentration generally takes on a constant steady-state value during the process. Thus, Eq. (18) can be simplified with k' taking the form of an apparent pseudo
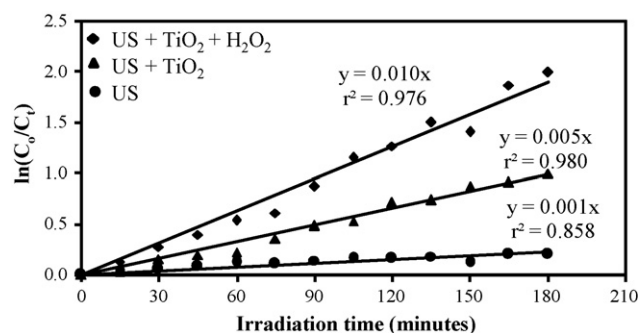
Fig. 10. The reaction kinetics plot for the sonocatalytic degradation of congo red.

first-order constant (k_{app}) as shown below.

$$-r = \frac{d}{dt}[\text{congo red}] = k_{app}[\text{congo red}] \quad (19)$$

where, $\quad k_{app} = k'[^{\bullet}OH] \quad (20)$

By integrating Eq. (19), a new equation relating the concentration to the reaction time can be obtained and it is given as Eq. (21).

$$\ln \frac{C_o}{C_t} = k_{app}t \quad (21)$$

or,

$$C_t = C_o e^{-k_{app}t} \quad (22)$$

where, C_o and C_t is the initial concentration and the concentration of the congo red at time t, respectively (mg/L), t is the ultrasonic irradiation time and k_{app} is the pseudo first-order constant (mg/L/min).

Plots of $\ln(C_o/C_t)$ versus time (t) for the three cases considered can be approximated as straight lines as shown in Fig. 10. The figure implies that the sonocatalytic degradation of congo red satisfactorily fitted the pseudo first-order kinetics. Thus, the slope of the linear lines should be equal to the apparent first-order rate constant (k_{app}). The k_{app} values and corresponding regression coefficients (r^2) are listed in Table 3. It is noted that sonocatalytic reaction was about five times higher than that of sonolysis and the highest k_{app} values was obtained with the combination of ultrasonic irradiation, TiO$_2$ sonocatalyst and H$_2$O$_2$. The combined process had a reaction rate of about one order of magnitude higher than that of sonolysis.

3.8. Reusability study of TiO$_2$ catalyst

The performance of used sonocatalysts and changes in their characteristics after the ultrasonic-assisted degradation of organics are hardly reported in previous publications. Therefore, an attempt was made in this study to elucidate the differences between the fresh and used TiO$_2$ and the consequences to the catalytic activity. Fig. 11 shows the degradation efficiency of congo red by the reused TiO$_2$ sonocatalyst with that of the fresh sonocatalyst as the reference. It is noted that the degradation efficiency of the reused TiO$_2$ catalyst was lower by merely about 10%. This result could be explained by the differences in the surface characteristics, crystal structures or particle size distribution between the fresh and used TiO$_2$ sonocatalyst under ultrasonic irradiation. The effects on the

Table 3
Rate coefficients for the sonocatalytic degradation of congo red under various conditions.

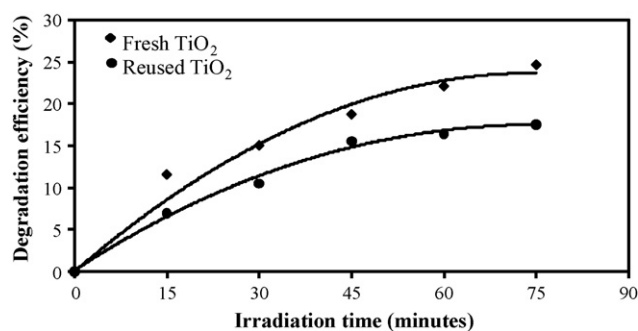| Experiment condition	k_{app} (min^{-1})	r^2
Ultrasonic only	0.001	0.858
Ultrasonic + TiO$_2$	0.005	0.980
Ultrasonic + TiO$_2$ + H$_2$O$_2$	0.010	0.976

Fig. 11. Sonocatalytic degradation of congo red by the fresh and reused TiO$_2$ catalysts (initial concentration = 10 mg/L, TiO$_2$ loading = 1.5 g/L).

characteristics of the sonocatalysts were attributed to the violent mechanical force imparted by the movement of the liquid on the surface of the solid particles leading to their partial disintegration.

In order to study of the effect of ultrasound irradiation on the particle size distribution of the TiO$_2$ sonocatalyst during the degradation of congo red, the spent TiO$_2$ sample was analyzed using a CILAS 1180 series particle size analyzer. The smallest detection limit for the particle size by this instrument was 0.04 μm. The normal size distribution plots for the fresh TiO$_2$ sonocatalyst and the used one are shown in Fig. 12(a) and (b), respectively. Both figures show that the size of the TiO$_2$ catalyst ranged between 0.04 and 1.50 μm. However, the highest cumulative value for the particle reduced from about 0.6 to 0.4 μm after the reaction. Correspond-
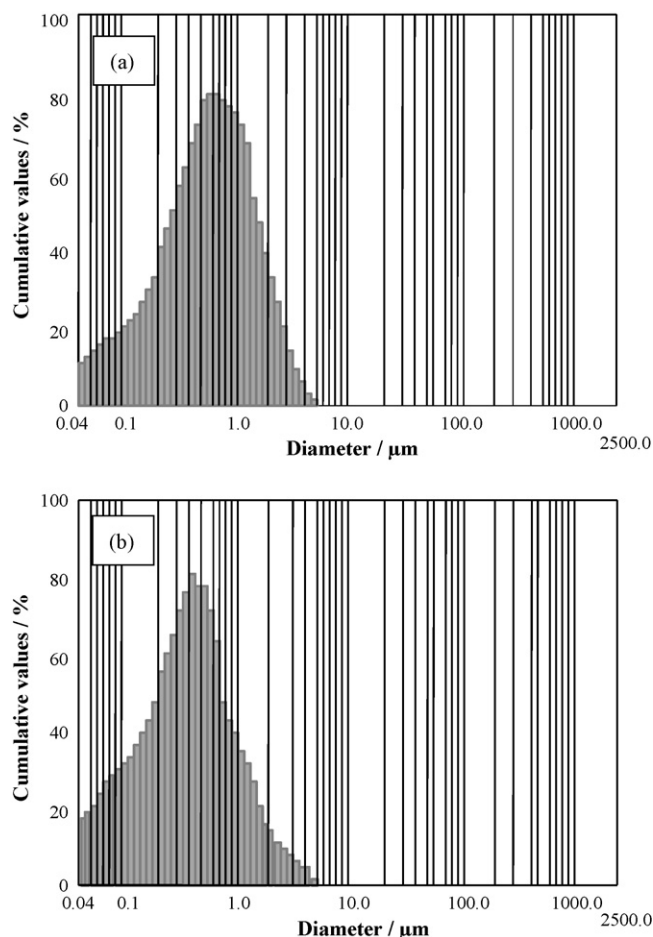

Fig. 12. Particle size distribution of the heat-treated TiO$_2$ catalyst at 800 °C for 2 h (a) before ultrasonic irradiation and, (b) after ultrasonic irradiation for 75 min.

ingly, the mode values (calculated by the system) of the particle sizes of heat-treated TiO_2 catalysts before and after ultrasonic irradiation occurred at the range between 0.3–1.1 μm and 0.2–0.7 μm, respectively. It is also observed that the cumulative values of the higher end (near 1.5 μm) of the distribution significantly reduced while that of the lower end (near 0.04 μm) significantly increased. All these observation suggested the partial disintegration of the sonocatalyst particles after the ultrasonic irradiation. This disintegration could reduce the micro and mesopores at the interstices of the particles leading to lower surface area for contact with the ultrasonic wave. However, as the ultrasonic wave was also expected to 'grind' the sonocatalyst particles, some new surface was expected to be available for the reaction [11]. Therefore, the overall result on the catalytic activity was basically governed by the balance between these two mechanisms.

The observations made in this study were consistent with a report by Hagenson and Doraiswamy [26]. They found that sonicating resulted in a significant reduction in the size of inorganic solids. The time required to reach a minimum particle size range was dependent the properties of the solid and the sonochemical equipment used. Despite better interaction with liquid medium during the ultrasonic degradation process, smaller particles are difficult to manage and they tend to form stable suspension and difficult to be separated out from the reaction system.

4. Conclusions

The phase transformation temperature from anatase to rutile by heat treatment method started to occurred at 800 °C and was more significant at 1000 °C, forming about 27.7% rutile phase in 4 h. It was found that anatase TiO_2 with minimal amount rutile phase demonstrated significantly better sonocatalytic activity than pure anatase. This was attributed to the ability of rutile to avoid hole-electron recombination. However, particle agglomeration at high temperature also caused the loss of surface area for efficient contact with the solution while the embedded rutile phase within the mass of TiO_2 could not participate in the reaction. The degradation of organic dyes (congo red, methylene blue and methyl orange) depended on the sonocatalysts' characteristics, dyes' chemical structures and their molecular weight. Congo red exhibited the higher sonocatalytic degradation efficiency. The highest sonocatalytic degradation efficiency for congo red (80% within 180 min) occurred at a dye initial concentration of 10 mg/L, TiO_2 loading of 1.5 g/L and the added H_2O_2 concentration of 450 mg/L. The sonocatalytic degradation process followed a pseudo first-order kinetics. The applicability of the model was demonstrated for the sonolytic, sonocatalytic and hydrogen peroxide-assisted sonocatalytic systems. Reused TiO_2 sonocatalyst showed a reduced congo red dye removal efficiency by about 10%. Meanwhile, the ultrasonic effect resulted in the significant disintegration of the sonocatalyst particles and the net effect on the activity was governed by the disappearance of existing active surface area and the emergence of new surface area that resulted.

Acknowledgements

References

[1] K. Selvam, K. Swaminathan, K.S. Chae, Microbial decolorization of azo dyes and dye industry effluent by Fomes lividus, World J. Microbiol. Biotechnol. 19 (6) (2003) 591–593.

[2] R. Vinu, G. Madras, Kinetics of sonophotocatalytic degradation of anionic dyes with nano-TiO₂, Environ. Sci. Technol. 43 (2009) 473–479.

[3] J. Wang, T. Ma, Z.H. Zhang, X.D. Zhang, Y.F. Jiang, Z.J. Pan, F.Y. Wen, P.L. Kang, P. Zhang, Investigation on the sonocatalytic degradation of methyl orange in the presence of nanometer anatase and rutile TiO₂ powders and comparison of their sonocatalytic activities, Desalination 195 (1–3) (2006) 294–305.

[4] J. Wang, Y.F. Jiang, Z.H. Zhang, G. Zhang, T. Ma, W. Sun, Investigation on the sonocatalytic degradation of congo red catalyzed by nanometer rutile TiO₂ powder and various influencing factors, Desalination 216 (1–3) (2007) 196–208.

[5] N.H. Ince, G.T. Guyer, Impacts of pH and molecular structure on ultrasonic degradation of azo dyes, Ultrasonics 42 (1–9) (2004) 591–596.

[6] J. Wang, Z.J. Pan, Z.H. Zhang, X.D. Zhang, F.Y. Wen, T. Ma, Y.F. Jiang, L. Wang, L. Xu, P.L. Kang, Sonocatalytic degradation of methyl parathion in the presence of nanometer and ordinary anatase titanium dioxide catalysts and comparison of their sonocatalytic abilities, Ultrason. Sonochem. 13 (6) (2006) 493–500.

[7] M. Abbasi, N.R. Asl, Sonochemical degradation of basic blue 41 dye assisted by nanoTiO₂ and H₂O₂, J. Hazard. Mater. 153 (3) (2008) 942–947.

[8] Y.G. Adewuyi, Heterogeneous sonophotocatalytic oxidation processes for the treatment of pollutants in water, Environ. Sci. Technol. 39 (22) (2005) 8557–8570.

[9] N. Shimizu, C. Ogino, M.F. Dadjour, K. Ninomiya, A. Fujihira, K. Sakiyama, Sonocatalytic facilitation of hydroxyl radical generation in the presence of TiO₂, Ultrason. Sonochem. 15 (2008) 988–994.

[10] H.H. Huang, Photocatalytic degradation of monochlorobenzene in water by UV/TiO₂ process, Ph.D dissertation, Graduate Institude of Environmental Engineering, National Central University 2006.

[11] N. Shimizu, C. Ogino, M.F. Dadjour, T. Murata, Sonocatalytic degradation of methylene blue with TiO₂ pellets in water, Ultrason. Sonochem. 14 (2) (2007) 184–190.

[12] K.N.P. Kumar, Growth of rutile crystallites during the initial stages of anatase-to-rutile transformation in pure titania and in titania-alumina, Scripta Metall. Mater. 32 (6) (1995) 873–877.

[13] J. Wang, W. Sun, Z.H. Zhang, Z. Jiang, X.F. Wang, R. Xu, R.H. Li, X.D. Zhang, Preparation of Fe-doped mixed crystal TiO₂ catalyst and investigation of its sonocatalytic activity during degradation of azo fuchsine under ultrasonic irradiation, J. Colloid Interface Sci. 320 (1) (2008) 202–209.

[14] J. Wang, T. Ma, Z.H. Zhang, X.D. Zhang, Y.F. Jiang, W. Sun, R.H. Li, P. Zhang, Investigation on the transition crystal of ordinary rutile TiO₂ powder by microwave irradiation in hydrogen peroxide solution and its sonocatalytic activity, Ultrason. Sonochem. 14 (5) (2007) 575–582.

[15] I.N. Kuznetsova, V. Blaskov, L. Znaidi, Study on the influence of heat treatment on the crystallographic phases of nanostructured TiO₂ films, Mater. Sci. Eng. B 137 (1–3) (2007) 31–39.

[16] M. Papadaki, R.J. Emery, M.A. Abu-Hassan, A. Díaz-Bustos, I.S. Metcalfe, D. Mantzavinos, Sonocatalytic oxidation processes for the removal of contaminants containing aromatic rings from aqueous effluents, Sep. Purif. Technol. 34 (2004) 35–42.

[17] M.H. Priya, G. Madras, Kinetics of TiO₂-catalyzed ultrasonic degradation of rhodamine dyes, Ind. Eng. Chem. Res. 45 (2006) 913–921.

[18] J.F. Porter, Y.G. Li, C.K. Chan, The effect of calcination on the microstructural characteristics and photoreactivity of Degussa P-25 TiO₂, J. Mater. Sci. 34 (7) (1999) 1523–1531.

[19] E.J. Kim, S.H. Hahn, Microstructure and photoactivity of titania nanoparticles prepared in nonionic W:O microemulsions, Mater. Sci. Eng. A 303 (1–2) (2001) 24–29.

[20] H. Lachheb, E. Puzenat, A. Houas, M. Ksibi, E. Elaloui, C. Guillard, J.M. Herrmann, Photocatalytic degradation of various types of dyes (alizarin S, crocein orange G, methyl red, congo red, methylene blue) in water by UV-irradiated titania, Appl. Catal. B-Environ. 39 (1) (2002) 75–90.

[21] C. Hachem, F. Bocquillon, O. Zahraa, M. Bouchy, Decolourization of textile industry wastewater by the photocatalytic degradation process, Dyes Pigments 49 (2) (2001) 117–125.

[22] G.V. Buxton, C.L. Greenstock, W.P. Helman, A.B. Ross, Critical review of rate constants for reactions of hydrated electrons, hydrogen atoms and hydroxyl radicals (•OH/•O⁻) in aqueous solution, J. Phys. Chem. Ref. Data 17 (1988) 513–886.

[23] J. Wang, T. Ma, Z.H. Zhang, X.D. Zhang, J.F. Jiang, D.B. Dong, P. Zhang, Y. Li, Investigation on the sonocatalytic degradation of parathion in the presence of nanometer rutile titanium dioxide (TiO₂) catalyst, J. Hazard. Mater. B 137 (2) (2006) 972–980.

[24] C. Mircolucchiari, D. Valtermaurino, Fe (III)-enhanced sonochemical degradation of methylene blue in aqueous solution, Environ. Sci. Technol. 39 (22) (2005) 8936–8942.

[25] J. Hartmann, P. Bartels, U. Mau, M. Witter, W.V. Tumpling, J. Hofmann, E. Nietzschmann, Degradation of the drug diclofenac in water by sonolysis in presence of catalysts, Chemosphere 70 (3) (2008) 453–461.

[26] L.C. Hagenson, L.K. Doraiswamy, Comparison of the effects of ultrasound and mechanical agitation on a reacting solid-liquid system, Chem. Eng. Sci. 53 (1) (1998) 131–148.